DOI: https://doi.org/10.24425/amm.2025.156259

S. JUNARDI 01 , M.S. ZAKARIA 01,2,3* , N.F. HAYAZI 01,3 , L.H. IBRAHIM 01,6 , M.F.M. NAZERI 01,3 , R.M. NORDIN 04,5 , M.K. AFDHOL 07,8 , K. JEŻ 09 , KHAIRUL ANWAR ABDUL HALIM 01,2

FACTORIAL DESIGN OPTIMIZATION OF TiO2-INFUSED SUPERHYDROPHOBIC COATINGS FOR IMPROVED STEEL CORROSION PROTECTION

This study investigates the development of a superhydrophobic coating on steel substrates using a factorial design method, focusing on its anti-corrosion applications. The coating formulation includes palm slag, stearic acid, expanded polystyrene (EPS), and titanium dioxide (TiO₂), with the coating applied to metal substrates. The superhydrophobic properties were assessed through water contact angle measurements, achieving a high degree of water repellence. Surface roughness was analysed using a 3D profilometer, revealing hierarchical nanostructures that contribute to the coating's hydrophobicity. The optimized formulation demonstrated effective corrosion protection, making it suitable for various industrial applications. The use of factorial experimental design (FED) proved highly effective in identifying optimal levels for the coating components, enhancing its performance. This research offers valuable comprehension into the formulation and characterization of superhydrophobic coatings, with significant implications for their use in diverse environments.

Keywords: Superhydrophobic coatings; palm slag; expanded polystyrene; corrosion; open circuit potential

1. Introduction

Superhydrophobic coatings, characterized by their nanoscopic surface layers with strong water resistance, have garnered significant interest due to their wide-ranging industrial applications. These coatings can be fabricated using various materials and nanoparticles, including polymeric nanocomposites [1]. Inspired by natural examples such as lotus leaves and certain animals, these surfaces exhibit self-cleaning properties, limited adhesion, and reduced drag for liquid flow [2]. Natural superhydrophobic surfaces, with water contact angles exceeding 150°, have attracted substantial research interest for their potential industrial applications as highlighted by [3]. Recent advancements have seen the development of superhydrophobic surfaces through diverse techniques such as spraying, chemical etching, lithography, electrospinning, surface wrinkling, chemical vapor deposition, layer-by-layer coating, and photolithography laser surface treatment [4].

One attribute that characterizes the non-wetting nature of material surfaces is superhydrophobicity [5]. Superhydrophobic surfaces offer excellent corrosion resistance by minimizing the contact area between liquids and the coated surface, making them suitable for applications in self-cleaning, anti-icing, oil-water separation, and notably, corrosion prevention [6]. This multidisciplinary field bridges wetting science and traditional corrosion research [7]. The superhydrophobic Lotus state can protect substrates from corrosion by forming an insulating air layer on the surface [8].

This study explores the development of superhydrophobic coatings using recycled materials, including expanded polystyrene foam and oil palm slag. The coatings were formulated using a factorial experimental design (FED) and their properties were evaluated with a 3D surface profilometer. Additionally, their corrosion protection performance was assessed through open circuit potential (OCP) testing, highlighting the potential of using recycled materials to create effective superhydrophobic coatings for corrosion protection.

- UNIVERSITI MALAYSIA PERLIS (UNIMAP), FACULTY OF CHEMICAL ENGINEERING & TECHNOLOGY, ARAU 02600, MALAYSIA
- UNIVERSITI MALAYSIA PERLIS (UNIMAP), CENTER OF EXCELLENCE GEOPOLYMER AND GREEN TECHNOLOGY (CEGEOGTECH), ARAU 02600, MALAYSIA
- UNIVERSITI MALAYSIA PERLIS (UNIMAP), SIG SURFACE TECHNOLOGY, ARAU 02600, MALAYSIA UNIVERSITI TEKNOLOGI MARA, FACULTY OF APPLIED SCIENCES, DEPARTMENT OF CHEMISTRY, PERLIS BRANCH ARAU CAMPUS, 02600 ARAU, PERLIS, MALAYSIA
- UNIVERSITI TEKNOLOGI MARA, GREEN AND FUNCTIONAL POLYMER RESEARCH GROUP, 40450 SHAH ALAM, SELANGOR, MALAYSIA ADVANCED POLYMER RESEARCH GROUP, CENTER OF EXCELLENCE GEOPOLYMER AND GREEN TECHNOLOGY (CEGEOGTECH), MALAYSIA
- UNIVERSITAS ISLAM RIAU, FACULTY OF ENGINEERING, DEPARTMENT OF PETROLEUM ENGINEERING, JALAN KAHARUDDIN NASUTION NO. 113, SIMPANGTIGA, PEKANBARU,
- INDONESIA UNIVERSITAS ISLAM RIAU, DEPARTEMENT OF RESEARCH AND STUDY PT. DURAZID VIDYA DAKSA, JALAN SISINGAMANGARAJA NO. 45A BANGKINANG, KAMPAR, INDONESIA
- CZESTOCHOWA UNIVERSITY OF TECHNOLOGY, FACULTY OF CIVIL ENGINEERING, 3 KAKADEMICKA STR., 42-218 CZESTOCHOWA, POLAND
- Corresponding author: salihin@unimap.edu.my



© 2025. The Author(s). This is an open-access article distributed under the terms of the Creative Commons Attribution License (CC-BY 4.0). The Journal license is: https://creativecommons.org/licenses/by/4.0/deed.en. This license allows others to distribute, remix, modify, and build upon the author's work, even commercially, as long as the original work is attributed to the author.

2. Experimental materials and method

Palm slag, sourced from Felda Palm Industries Sdn Bhd, Malaysia, was used as a filler. Ethanol (95%) was obtained from Systerm®, ethyl acetate (99.8%) from Sigma-Aldrich®, stearic acid from Fluka® Analytical, and titanium dioxide from Huntsman Corporation. The formulation was developed using a central composite design (CCD) within a factorial experimental design (FED), implemented via Design-Expert® software (Version 13, Stat-Ease, USA) as shown in TABLE 1.

For filler preparation, palm slag and titanium dioxide were mixed with distilled water in a 1:10 ratio and stirred at 90°C. Stearic acid was mixed with ethanol, heated until dissolved, and combined with the filler solution, then stirred for 3 hours. The matrix involved diluting expanded polystyrene foam (EPS) with ethyl acetate. After 3 hours, the diluted EPS was mixed with the filler solution for 15 minutes before applying the coating onto the substrate. Prior to the coating application, mild steel sheets were cut into 75 mm × 25 mm × 3 mm pieces, degreased thoroughly with acetone, and dried. The test pieces were then abraded on the test sides with 180-grade silicon carbide paper and wiped with petroleum spirits to remove any contaminants.

Water contact angles were measured by dripping distilled water onto the sample surface and photographing droplets with a Nikon D3200. ImageJ software analyzed the contact angles. Surface roughness was assessed using a 3D surface profiler (Pemtron, Hawk 3D Wt-250), and images were processed with a scanning probe image processor (SPIP) for topographical analysis.

TABLE 1
The composition formulation for preparation of superhydrophobic coating

Sample	Palm Slag	Stearic Acid	EPS	TiO ₂
SI SI	-1	-1	+1	-1
S2	0	0	0	0
S3	+1	-1	+1	+1
S4	0	0	0	0
S5	-1	+1	-1	-1
S6	+1	+1	-1	+1
S7	0	0	0	0
S8	-1	+1	+1	-1
S9	0	0	0	0
S10	+1	+1	-1	-1
S11	-1	+1	-1	+1
S12	-1	-1	+1	+1
S13	+1	+1	+1	-1
S14	-1	+1	+1	+1
S15	+1	-1	+1	-1
S16	+1	-1	-1	-1
S17	+1	+1	+1	+1
S18	+1	-1	-1	+1
S19	-1	-1	-1	+1
S20	-1	-1	-1	-1
S21	0	0	0	0
S22	0	0	0	0

^{*} Indicator: +1 = High, 0 = Center, -1 = Low

Open circuit potential (OCP) assessed the corrosion behavior of the superhydrophobic coating, using a saturated calomel electrode (SCE) as a reference and a multimeter to measure potential values, providing insights into the coating's performance under specific conditions.

3. Results and discussion

3.1. Chemical composition of palm slag

TABLE 2 displays the chemical composition of palm slag, determined by X-ray fluorescence spectroscopy. Silicon dioxide (SiO₂) dominates, accounting for 71.8% of the slag's composition. Other chemical compositions include calcium oxide, magnesium oxide, sulfur trioxide, potassium oxide, phosphorus pentoxide, titanium dioxide, and iron oxide (Fe₂O₃).

 $\label{eq:table 2} TABLE\ 2$ The chemical composition of palm slag by XRF

Chemical Composition	Palm Slag (%)
SiO ₂	71.8
Al_2O_3	5.48
Fe ₂ O ₃	5.57
CaO	4.6
MgO	1.4
SO ₃	0.16
K ₂ O	8.21
P_2O_5	1.92
TiO ₂	0.396

3.2. Water Contact Angle

The water contact angle is a crucial measure of a material's wettability, determining the contact angle between a material and a water droplet. Superhydrophobic surfaces have high water repellence, with contact angles exceeding 150 degrees. TABLE 3 shows that S17's formulation achieves superhydrophobicity, with a water contact angle of 151.25 degrees. Stearic acid and titanium dioxide have the greatest effect on superhydrophobic properties, as they repel water and create an abrasive surface. S3 has the smallest water contact angle, with the lowest concentration of stearic acid, indicating a less hydrophobic surface. This is due to the presence of stearic acid molecules creating a hydrophobic barrier, preventing water from saturating the surface.

3.3. Surface Roughness Analysis

A 3D nano profiler was utilized to measure surface roughness using 3D roughness characteristics. The results showed that the superhydrophobic coating for formulation S17 had a maximum height of 294498.656 nm and an average height of 138269.473 nm. This rough surface was due to microporous

Water contact angle for each formulation

TABLE 3

Sample	Palm Slag	Stearic Acid	EPS	TiO ₂	Water Contact Angle (WCA)
S1	-1	-1	+1	-1	120.47
S2	0	0	0	0	133.10
S3	+1	-1	+1	+1	114.85
S4	0	0	0	0	130.30
S5	-1	+1	-1	-1	137.90
S6	+1	+1	-1	+1	134.55
S7	0	0	0	0	137.54
S8	-1	+1	+1	-1	132.47
S9	0	0	0	0	137.63
S10	+1	+1	-1	-1	130.84
S11	-1	+1	-1	+1	134.67
S12	-1	-1	+1	+1	139.20
S13	+1	+1	+1	-1	130.95
S14	-1	+1	+1	+1	128.94
S15	+1	-1	+1	-1	133.28
S16	+1	-1	-1	-1	136.27
S17	+1	+1	+1	+1	151.25
S18	+1	-1	-1	+1	124.65
S19	-1	-1	-1	+1	138.83
S20	-1	-1	-1	-1	125.74
S21	0	0	0	0	131.16
S22	0	0	0	0	133.81

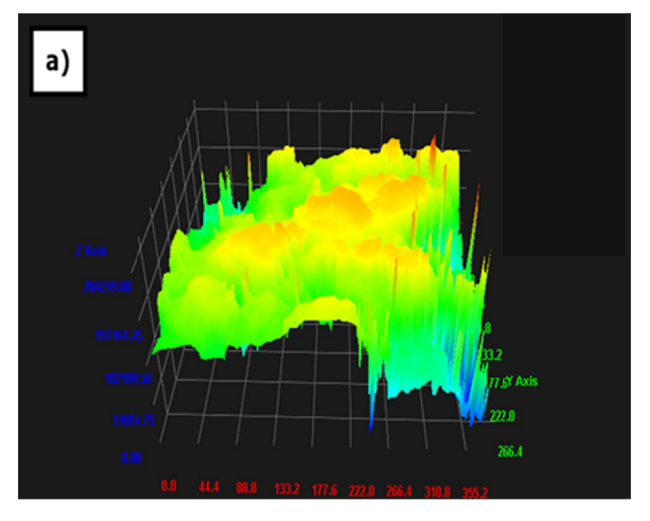
^{*} Indicator: +1 = High, 0 = Center, -1 = Low

feature structures and protuberances, resulting in a rough surface. The maximum height of S17 indicates significant differences, such as pits, protrusions, or deep scratches, which may impact a component's performance or functionality. Superhydrophobicity benefits from roughness, as it traps air and prevents water from adhering to the surface. This results in a highly hydrophobic surface, as shown in Fig. 1.

TABLE 4 Specification data: height, area size and pitch of the S17

Item	Value		
Start Pos (um)	X:84.36 Y:38.48		
Area Size (um)	377.40 x 285.64		
Center Pos (um)	X:272.32 Y:180.56		
Pitch (um)	1.480		
Minimum Height (nm)	-24167.695		
Maximum Height (nm)	294489.656		
Average Height (nm)	138269.473		

Surface roughness plays a crucial role in wetting liquid droplets on solid surfaces. A 3D nano profiler was used to characterize surface topography at the nanoscale, revealing significant differences in average roughness (Ra) and root mean square roughness (Rq). The surface roughness of a sample exhibited hierarchical nanostructures, which varied depend-



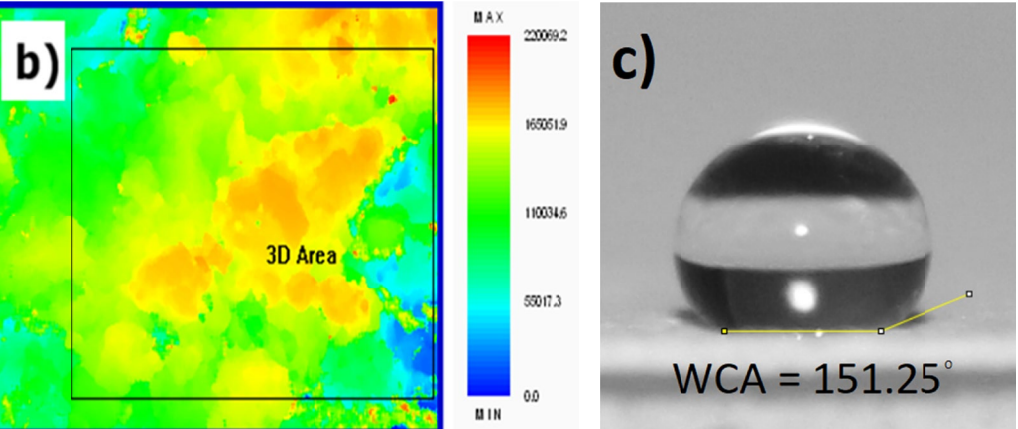


Fig. 1. 3D nano profiler imaging for (a) 3D view of S17 (b) 2D View and (c) the contact angle of S17

ing on the scanned region's size. The waviness of the sample had various features that changed depending on the size of the scanned region. S17's surface coating had a maximum roughness of 294489.656 nm and a maximum waviness of 849.25 nm as displayed in Fig. 2, displaying multiscale features, with wavy patterns representing microstructures and roughness factor representing nanostructures. This aligns with [9] findings that the superhydrophobic surface was impacted by two factors: wavy features representing microstructures and roughness factor representing nanostructures.

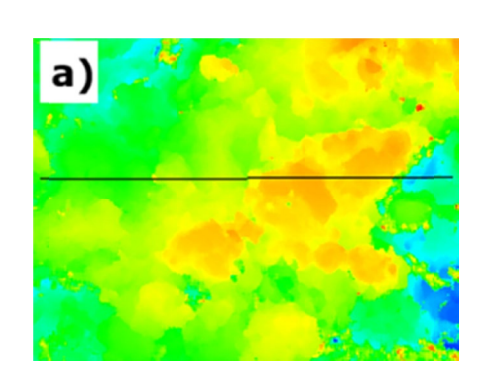




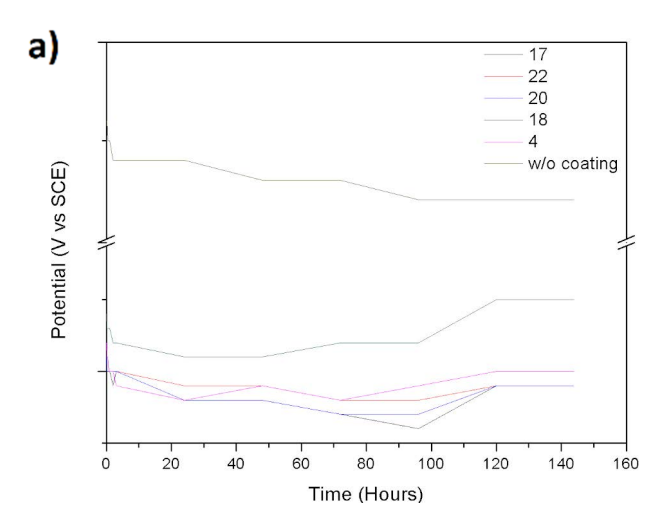


Fig. 2. 2D view for (a) S17, surface roughness (b) and waviness (c) based on the black line shown in 2D image

3.4. Corrosion Protection Performances

The Pourbaix diagram shows that S17 has the most significant corrosion resistance, as demonstrated by comparing the readings from the standard hydrogen electrode (SHE) to the Fe Pourbaix diagram. The SHE potential value is distant from the corrosion zone and immunity region, indicating that all 5 coatings found in the immunity region exhibit extraordinary corrosion resistance as shown in Fig. 3. Superhydrophobic coatings in the immunity area efficiently repel water and corrosive chemicals, reducing the chance of corrosion or deterioration. The immunity area in a Pourbaix diagram indicates that corrosion-

causing chemical or electrochemical processes will not affect the coating. Superhydrophobic coatings offer a substantial barrier against corrosion, preserving long-term stability and preventing corrosion in various situations, making them attractive for applications like maritime environments, industrial settings, and severe weather-sensitive infrastructure.



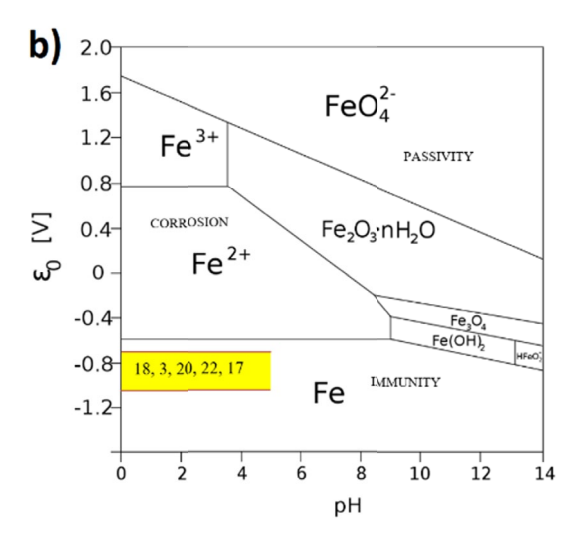


Fig. 3. a) Open circuit potential vs times curves and (b) Pourbaix diagram for Fe

3.5. Factorial Experimental Design

The study analyzed the results of experimental trials using Design-Expert® software and found that B and ABD are the most significant factors affecting superhydrophobic coatings stated in Fig. 4(a). The Pareto chart in Fig. 6(b) showed that the ABD bar exceeded the Bonferroni limit, indicating a statistically significant effect on the response variable. The stearic acid (B) had a significant impact on the response, as the B bar fell within the Bonferroni and t-value limits. The t-value limit determines the magnitude and significance of stearic acid's specific effect. Although EPS has no significant effect on the response, it does affect the level of coating adhesion and the difficulty of coating application.

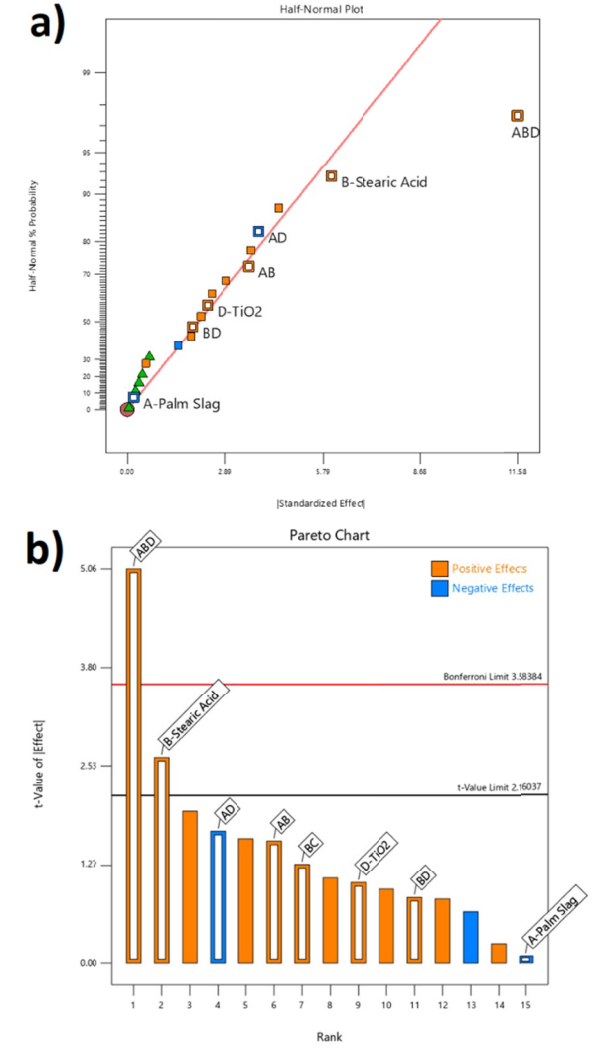


Fig. 4. a) Half-normal % probability plot and (b) Pareto chart for screening the most important factor influencing the water contact angle (A) palm slag, (B) stearic acid, (C) EPS and (D) TiO₂

Meanwhile, the graph in Fig. 5 shows the interaction between stearic acid and wettability response, with contact angle measuring the surface's wettability response. The study used ethanol solvent and ethyl acetate as control variables. Increased stearic acid increased the water contact angle for a superhydrophobic coating, resulting in good superhydrophobicity. The interaction of ACD, palm slag, stearic acid, and TiO₂ was also examined.

TABLE 5 displays the ANOVA response of water contact angle of the superhydrophobic coating. The model is significant with a 4.42 F-value, with a 1.19% probability of noise. P-values below 0.05 indicate significant model terms, such as B and ABD. Values above 0.1000 indicate insignificant terms, and a 3.35 Lack of Fit F-value suggests the model adequately explains the observed data, with no significant misfit indications.

TABLE 6 shows the fit statistic for factorial experimental design (FED). A negative predicted R2 suggests the aggregate mean may be more accurate than the existing model. Adequate precision is preferred, with a 7.859 signal-to-noise ratio.

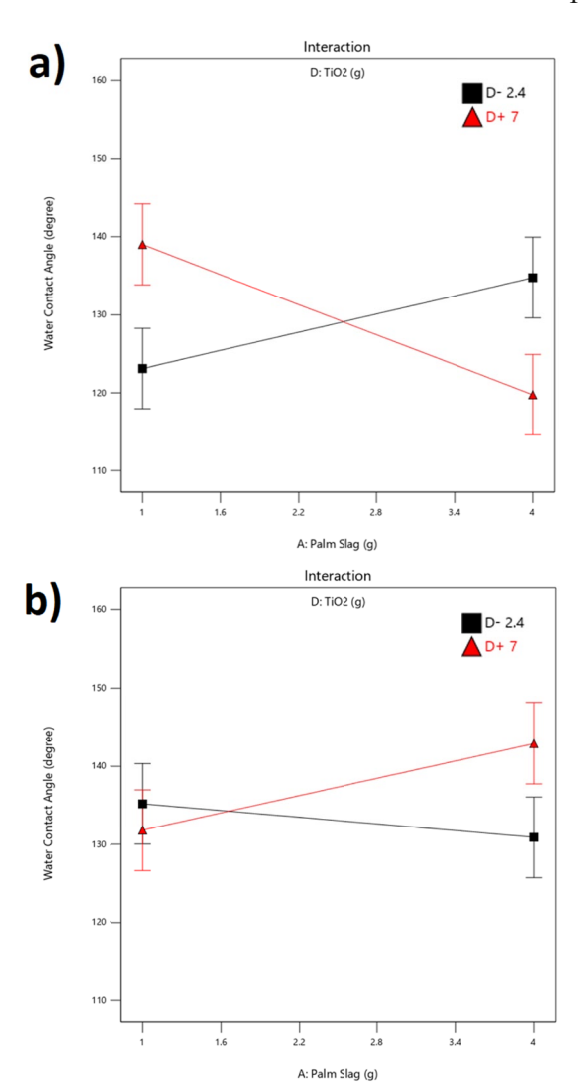


Fig. 5. (a) Interaction of AD in lowest amount of stearic acid and (b) highest amount of stearic acid to the response

TABLE 5
ANOVA response of water contact angle

Source	Sum of Squares	df	Mean square	F-value	P-Value	
Model	874.96	9	97.22	4.42	0.0119	significant
A-Palm Slag	0.1556	1	0.1556	0.0071	0.9345	
B-Stearic Acid	145.70	1	145.70	6.62	0.0259	significant
C-EPS	9.08	1	9.08	0.4125	0.5339	
D-TiO ₂	22.57	1	22.57	1.03	0.3329	
AB	51.83	1	51.83	2.36	0.1531	
AD	60.44	1	60.44	2.75	0.1256	
BC	34.04	1	34.04	1.55	0.2394	
BD	15.00	1	15.00	0.6820	0.4265	
ABD	536.15	1	536.15	24.37	0.0004	significant
Curvature	13.28	1	13.28	0.6036	0.4536	
Residual	242.02	11	22.00			
Lack of Fit	193.80	6	32.30	3.35	0.1029	not significant
Pure Error	48.21	5	9.64			
Cor Total	1130.26	21				

Statistical Parameters	Value
Standard Deviation	4.69
Mean	132.65
Coefficient of variance percentage	3.54
R ²	0.7833
Adjusted R ²	0.6061
Predicted R ²	-0.2960
Adequate Precision	7.8589

Fit statistics

4. Conclusion

The study successfully developed a superhydrophobic coating on steel substrates using a factorial experimental design (FED) to optimize the formulation. The optimal levels of key components were identified as high concentrations of palm slag, stearic acid, expanded polystyrene (EPS), and titanium dioxide (TiO₂), as demonstrated in formulation S17. This formulation achieved a water contact angle of 151.25 degrees, indicating exceptional water repellency. The synergistic effects of stearic acid and TiO2 significantly enhanced the superhydrophobic properties by creating an abrasive surface. The optimized formulation also exhibited outstanding corrosion resistance, as shown by its position in the immunity region of the Pourbaix diagram. These findings highlight the potential of using recycled materials, such as palm slag and EPS, in creating effective superhydrophobic coatings for industrial applications, paving the way for future research and development in protective coatings.

Acknowledgments

The authors would like to express their gratitude and acknowledge the support from the Fundamental Research Grant Scheme (FRGS) under grant number FRGS/1/2020/TK0/UNIMAP/03/24 from the Ministry of Higher Education Malaysia.

REFERENCES

- [1] S. Barthwal, S. Uniyal, S. Barthwal, Micromachines **15** (3), 391 (2024). DOI: https://doi.org/10.3390/mi15030391
- [2] M. Shigrekar, V. Amdoskar, RSC Adv. 14 (44), 32668-32699 (2024). DOI: https://doi.org/10.1039/d4ra04767b
- [3] M.Z. Khan, J. Militky, M. Petru, B. Tomková, A. Ali, E. Tören,
 S. Perveen, Eur. P olym. J. 178, 111481 (2022).
 DOI: https://doi.org/10.1016/j.eurpolymj.2022.111481
- [4] J. Fu, X. Liao, Y. Ji, Y.Mo, L.L. Zhang, Mar. Sci. Eng. 12 (10), 1741 (2024). DOI: https://doi.org/10.3390/jmse12101741
- Z. Belamri, L. Chetibi, Arch. Metall. Mater. 69, 1097-1106 (2024).
 DOI: https://doi.org/10.24425/amm.2024.150930
- [6] Y. Ge, J. Cheng, L. Xue, B. Zhang, P. Zhang, X. Cui, S. Hong, Y. Wu, X. Zhang, X. Liang, RSC Adv. 12 (51), 32813-32824 (2022). DOI: https://doi.org/10.1039/d2ra06073f
- [7] M. Cui, B. Wang, Z. Wang, Adv. Eng. Mater. 21 (7), 1801379 (2019). DOI: https://doi.org/10.1002/adem.201801379
- [8] E. Vazirinasab, R. Jafari, G. Momen, Surf. Coat. Technol. 341, 40-56 (2018).
 DOI: https://doi.org/10.1016/j.surfcoat.2017.11.053
- [9] P. Nguyen-Tri, N.H. Tran, C.O. Plamondon, L. Tuduri, D.V.N. Vo, S. Nanda, A. Mishra, H.P. Chao, A.K. Bajpai, Prog. Org. Coat. 132, 235-256 (2019).

DOI: https://doi.org/10.1016/j.porgcoat.2019.03.042